OPEN

Support Vector Machines Model of Computed Tomography for Assessing Lymph Node Metastasis in Esophageal Cancer with Neoadjuvant Chemotherapy

Zhi-Long Wang, MD, Zhi-Guo Zhou, PhD,† Ying Chen, MD,* Xiao-Ting Li, MD,* and Ying-Shi Sun, MD**

Objective: The aim of this study was to diagnose lymph node metastasis of esophageal cancer by support vector machines model based on computed tomography.

Materials and Methods: A total of 131 esophageal cancer patients with preoperative chemotherapy and radical surgery were included. Various indicators (tumor thickness, tumor length, tumor CT value, total number of lymph nodes, and long axis and short axis sizes of largest lymph node) on CT images before and after neoadjuvant chemotherapy were recorded. A support vector machines model based on these CT indicators was built to predict lymph node metastasis.

Results: Support vector machines model diagnosed lymph node metastasis better than preoperative short axis size of largest lymph node on CT. The area under the receiver operating characteristic curves were 0.887 and 0.705, respectively.

Conclusions: The support vector machine model of CT images can help diagnose lymph node metastasis in esophageal cancer with preoperative chemotherapy.

Key Words: support vector machine, computed tomography, esophageal cancer, lymph node metastasis

(*J Comput Assist Tomogr* 2017;41: 455–460)

The prognosis of patients with resectable esophageal cancer remains poor. The reported 5-year survival rates range from 20 to 36% after intentionally curative surgery.[1–3] Median survival is only 9–24 months in patients with surgical treatment.[4–9] Prospective randomized trials demonstrated an improved survival after neoadjuvant therapy compared to surgery alone in patients with esophageal cancer. Some important studies include the CROSS trial, which analyzed neoadjuvant chemoradiation for patients with esophageal adenocarcinoma or squamous cell carcinoma, and the MAGIC and French trials analyzing neoadjuvant chemotherapy for adenocarcinoma.[10–12] Data from the FFCD9901 study suggested preoperative chemoradiotherapy increases complication incidence and mortality.[13] Therefore, preoperative chemotherapy in treating esophageal carcinoma is gradually accepted by surgeons.

As reported by Worldwide Esophageal Cancer Collaboration, survival decreases with the presence of lymph node metastases (LNM).[14] Indeed, the lymph node category was shown to be an independent prognostic factor in lymph node positive patients with resectable thoracic esophageal cancer.[15] Imaging examinations are the most commonly used tools for lymph node status evaluation in esophageal cancer. Wakelin et al compared computed tomography (CT), laparoscopic ultrasound, and endoscopic ultrasound (EUS) in the preoperative staging of esophagogastric carcinoma; the accuracy of CT in diagnosing the N stage of esophageal cancer was 17 of 29 (59%).[16] These authors concluded that the nodal status remains the most difficult area to assess using all three modalities. The main hurdle appeared to be the differentiation between benign and malignant enlarged nodes, with lymph node size alone not being a good criterion for assessing malignancy.

In recent years, machine-learning methods have been used to predict complex biological problems. Support vector machines (SVMs) are supervised machine learning techniques widely used in pattern recognition and classification problems. An SVM algorithm performs a classification by constructing a multidimensional hyperplane that optimally discriminates between two classes, by maximizing the margin between two data clusters. This algorithm achieves high discriminative power by using special nonlinear functions called kernels to transform the input space into a multidimensional space.[17] SVMs have been used in medical applications.[18–20] Given a set of training cases, each marked as belonging to one of two categories, a SVM training algorithm builds a model that predicts whether a new case falls into one category or the other.

Therefore, we used CT imaging data before and after neoadjuvant chemotherapy to establish a SVM mathematical model. In addition, the diagnostic power of the SVM method for differentiating LNM in patients with esophageal cancer was assessed. Because squamous cell carcinomas are significantly more common than adenocarcinomas and other malignant esophageal cancers in Asians, only patients with squamous cell carcinomas were evaluated in this study.

MATERIALS AND METHODS

Patients

This retrospective study was approved by the Ethics Committee of our hospital, with a waiver of requirement for informed

From the *Key Laboratory of Carcinogenesis and Translational Research (Ministry of Education), Department of Radiology, Peking University Cancer Hospital & Institute, Beijing, China; and †Department of Radiation Oncology, The University of Texas Southwestern Medical Center, Dallas, Texas.

Received for publication July 2, 2016; accepted August 16, 2016.

Correspondence to: Ying-Shi Sun, MD, Peking University Cancer Hospital & Institute, No. 52, Fucheng Road, Haidian District, Beijing, 100142, China (e-mail: sys27@163.com).

Funding: This work was supported by the National Natural Science Foundation of China (grant no. 81471640), the National Basic Research Program of China (973 Program) (grant no. 2011CB707705), and Beijing Health System High Level Health Technical Personnel Training Plan (No. 2013-3-083).

The authors declare no conflict of interest.

Authors' contributions: ZLW and YSS were guarantors of integrity of the entire study. ZLW carried out the study design and manuscript editing. ZGZ and YC carried out the data analysis. YSS participated in the manuscript preparation. XTL carried out the statistical analysis. All authors read and approved the final manuscript.

DOI: 10.1097/RCT.0000000000000555

consent. The clinical data were collected from the prospective database of our hospital. All patients in this database who had pathologically confirmed esophageal squamous cell carcinoma and received preoperative chemotherapy from January 2006 to January 2012 were included. All patients underwent gastroscopy to acquire pathological information, and received baseline and preoperative enhanced CT examinations.

Exclusion criteria were (a) pathologically proven adenocarcinoma, small cell carcinoma, mixed cancer, or other diseases; (b) other preoperative therapies (e.g., radiotherapy) simultaneously; (c) esophageal multiple primary carcinoma; (d) death within 30 days after surgery; (e) enhanced CT data before preoperative chemotherapy not obtained or images not interpretable; and (f) non-suitability for radical esophagectomy because of tumor progression or patient's physical condition.

CT Protocol

MDCT was performed using a 64–detector row CT scanner (LightSpeed 64; GE Healthcare, Milwaukee, WI). Chest unenhanced CT scans were acquired with 0.625 mm collimation, 120–140 kVp, and 300–350 mAs. Subsequently, a total of 100 ml iopromide (Ultravist; Schering, Berlin, Germany) was administered intravenously via an 18-gauge angiographic catheter inserted into an antecubital vein, at 3 mL/sec with an automatic injector. Contrast-enhanced CT scans were performed at 60 seconds after iopromide injection. Sagittal and coronal reconstructions were carried out with contrast-enhanced images.

Image Analysis

Baseline and preoperative CT images were analyzed using the picture archiving communication system (PACS) by two independent radiologists blinded to patients' clinical history. The following CT indicators were measured:

Tumor length: longest diameter obtained from the sagittal CT image.

Tumor thickness: lesion thickness obtained from the axial CT image.

Tumor CT value: region of Interest (ROI) placed on the lesion with maximum cross-section at the cross-sectional CT image.

Total LN number: number of all visible regional lymph nodes on Chest CT image.

Long axis size of largest regional LN (LSDL): long axis diameter of the largest regional lymph node in the axial CT image.

Short axis size of largest regional LN (SSDL). Diameter perpendicular to the long axis of the largest regional lymph node in the axial CT image.

The average results from the two radiologists were used for continuous variable analysis. Changes of CT image indicators between baseline and preoperative CT were assessed.

Statistical Analysis

LNM Assessment

All patients were divided into positive-LNM and negative-LNM groups, respectively. Node metastasis was confirmed by postoperative pathological results. A univariate statistical analysis with the SPSS software version 17.0 (SPSS Inc., Chicago, IL) was performed to evaluate the differences in various imaging indicators between the positive-LNM and negative-LNM groups. Group comparison was carried out by independent-samples T test. $P < 0.05$ was considered statistically significant.

The CT indicators significantly different between positive-LNM and negative-LNM groups were selected to build the SVM model. Receiver operating characteristic (ROC) curves were used to evaluate these indicators in diagnosing LNM. The MedCalc software version 11.2 (MedCalc; MedCalc Software, Ghent, Belgium) was used to generate and compare the ROC curves.

Least Squares Support Vector Machine (SVM)

Least squares support vector machine (LS-SVM) was proposed by Suykens and Vandewalle.[21] Compared with other SVMs, LS-SVM utilizes quadratic sum of the slack variables as the penalty factor which ensures that LS-SVM can obtain a small training error. Specifically, LS-SVM minimizes the follow optimization problem, that is:

$$\begin{aligned} \min_{\mathbf{w},b,\mathbf{e}} \quad & \frac{1}{2}\mathbf{w}^T\mathbf{w} + \frac{\gamma}{2}\sum_{i=1}^{N} e_i^2 \\ s.t. \quad & y_i[\mathbf{w}^T\phi(\mathbf{x}_i) + b] = 1 - e_i, \quad i = 1, \cdots, N \end{aligned}, \tag{1}$$

where $\mathbf{x}_i$ is the i-th training sample, $y_i \in \{-1,1\}$ is the label of $\mathbf{x}_i$, ϕ is a feature map which maps $\mathbf{x}_i$ to the feature space, $\mathbf{w}$ is the weight parameter vector, b is the bias parameter, e_i is i-th slack variable and $\mathbf{e} = (e_1, \cdots, e_N)^T$, γ is a tuning parameter which makes a trade-off between the slack variable penalty and the margin. The Lagrangian function of Eq. (1) is

$$L = \frac{1}{2}\mathbf{w}^T\mathbf{w} + \frac{\gamma}{2}\sum_{i=1}^{N} e_i^2 - \sum_{i=1}^{N} \alpha_i \left\{ \left[\mathbf{w}^T\phi(\mathbf{x}_i) + b\right] + e_i - y_i \right\}, \tag{2}$$

where α_i is i-th Lagrange multiplier ($i = 1, \cdots, N$). According to the optimal conditions, we have

$$\mathbf{w} = \sum_{i=1}^{N} \alpha_i \phi(\mathbf{x}_i), \tag{3}$$

$$\sum_{i=1}^{N} \alpha_i = 0, \tag{4}$$

$$\alpha_i = \gamma e_i, \tag{5}$$

and

$$y_i = \mathbf{w}^T\phi(\mathbf{x}_i) + b + e_i, i = 1, \cdots, N. \tag{6}$$

By eliminating $\mathbf{w}$ and $\mathbf{e}$, we can obtain the system of linear equations

$$\begin{bmatrix} 0 & \mathbf{1}^T \\ \mathbf{1} & \boldsymbol{\Omega} + \frac{1}{\gamma}\mathbf{I} \end{bmatrix} \begin{bmatrix} b \\ \boldsymbol{\alpha} \end{bmatrix} = \begin{bmatrix} 0 \\ \mathbf{y} \end{bmatrix}, \tag{7}$$

where $\boldsymbol{\alpha} = (\alpha_1, \cdots, \alpha_N)^T$, $\mathbf{y} = (y_1, \cdots, y_N)^T$, $\mathbf{1} = (1, \cdots, 1)^T$ is a length-N vector, $\mathbf{I}$ is $N \times N$ identity matrix, and $\boldsymbol{\Omega} = (\phi(\mathbf{x}_i)^T\phi(\mathbf{x}_j))_{N\times N}$ is Gram matrix. Solving Eq. (7), we obtain the solution b^* and $\boldsymbol{\alpha}^*$. Then the optimal weight parameter vector $\mathbf{w}^*$ can be computed by Eq. (3) and e_i by Eq. (5). For a testing sample $\mathbf{x}$, its label can be estimated by

$$sign(y) = sign\left(\mathbf{w}^T\phi(\mathbf{x}) + b\right), \tag{8}$$

LS-SVM can easily be extended to K-class ($K > 2$) classification problem by one-versus-one strategy.[22]

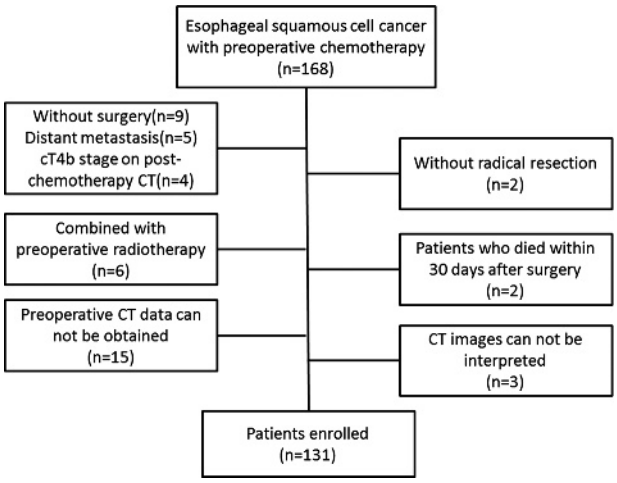

FIGURE 1. Flow chart of the study.

In this study, a free LS-SVM software package in MATLAB (version 7.0; MathWorks, Inc., Natick, MA) was applied to generate the SVM model. The default kernel function is used. A LS-SVM model for assessing LNM was established. Input indexes were the indicators obtained by the above univariate statistical analysis. The output index was lymph node metastasis in the patient. Confirmation was carried out by surgery and histopathology. Positive LNM was defined as 1 and negative LNM as −1. Fifty percent of cases were randomly selected to constitute the training sample. The remaining 50% of cases formed the testing sample. The training sample was used to establish the LS-SVM model. Finally, the ability of the model to predict LNM in the testing set and all cases was evaluated by ROC curves. ROC curves can be created automatically by the MATLAB software.

RESULTS

A total of 131 patients (102 males and 29 females; mean age of 58.0 years, ranging from 42 to 75 years) were included in the study (Fig. 1). There were 51 cases with lymph node metastasis and 80 without. The clinicopathological features of the patients are detailed in Table 1. The majority of patients (97%; 127/131) received a platinum-based two-drug combination, mainly paclitaxel (175 mg/m^2, IV, d1 Q21) and cisplatin (25 mg/m^2 IV, d1–3 Q21); the remaining patients received nedaplatin (80 mg/m^2) combined with paclitaxel. A total of one to four chemotherapy cycles were administered before surgery at 3–6 weeks after neoadjuvant chemotherapy.

In the univariate analysis, preoperative tumor thickness, preoperative long axis and short axis sizes of largest lymph node, total numbers of lymph nodes in baseline and preoperative CT, and change of tumor thickness in second CT showed statistically significant differences between the LNM positive and negative groups (Table 2). Of these six CT indicators, preoperative short axis size of largest lymph node yielded the highest power for diagnosing LNM in ROC curves (Table 3, Fig. 2), with an area under the ROC curve (AUC) of 0.705.

After the random sampling by the SPSS statistical software, 66 cases were randomly selected to constitute the training sample. The other 65 cases were defined as testing sample. The training sample was used to establish the LS-SVM model. When we use this model to predict the training sample and testing sample, the AUCs of the SVM model were 0.955 and 0.553, respectively (Fig. 3a, b). The AUC of the SVM model predicting all samples reached 0.887 (Fig. 3c).

By comparing the ROC curves, the SVM model performed significantly better than preoperative short axis size of largest lymph node ($P < 0.05$).

DISCUSSION

Lymph node metastasis affects the surgical treatment of patients with esophageal cancer, and is also an important prognostic factor. Currently, preoperative diagnosis mainly depends on various imaging methods. Yokota et al indicated that clinical node diagnosis has low specificity and negative predictive value for predicting pathological nodes in the preoperative diagnosis of lymph node metastasis for patients with locally advanced resectable esophageal cancer.[23]

Because metastatic lymph node detection on CT images mainly depends on size, the sensitivity and specificity of CT vary with the definition of an abnormally enlarged node. In general, intrathoracic and abdominal lymph nodes greater than 1 cm in diameter are considered to be enlarged, while supraclavicular lymph nodes with a short axis exceeding 5 mm are considered to be pathologic.[24]

Most studies using the common size criterion of 1 cm to define enlarged nodes report CT sensitivity of 30–60%, whereas specificity tends to be somewhat higher (60–80%).[25,26] In a study by Picus et al, nearly all metastatic peri-esophageal lymph nodes measuring less than 7 mm were indistinguishable from nonmetastatic lymph nodes by CT.[27] In addition, the presence of benign enlarged and inflammatory lymph nodes in esophageal cancer reduces the specificity of CT for detecting lymph node metastases. The lack of uniform criteria is the main constraint in predicting lymph node metastasis preoperatively.

The biological behavior of esophageal cancer reflects the histopathological performance of tumor malignancy and invasion. It affects lymph node metastasis directly or indirectly. The concrete manifestations of cancer biological behavior include, for example, tumor size, tumor invasion of other organs, lymph node metastasis, and distant metastasis. Therefore, MDCT imaging can accurately reflect the biological behavior of esophageal cancer histopathology. Univariate analysis in this study showed that all six indicators obtained from CT images were associated with LNM in esophageal cancer. Therefore,

TABLE 1. Patient Characteristics

Characteristics	Number	Percent
Sex		
Male	102	77.9%
Female	29	22.1%
Age (median, range)		58 (42–75)
Location		
Upper 1/3	35	26.7%
Middle 1/3	55	42.0%
Lower 1/3	41	31.3%
Surgical method		
Transhiatal	17	13.0%
Modified McKeown	98	74.8%
Modified Ivor-Lewis	10	7.6%
Modified Sweet	6	4.6%

TABLE 2. The Results of Univariate Statistical Analysis for CT Indicators of Baseline and Preoperative CT

	LNM (+)*	LNM (−)*	T value	*P*
Baseline CT				
Tumor thickness (mm)	17.6 + 6.2	17.2 + 6.1	0.369	0.713
Tumor length (mm)	7.7 + 2.3	7.3 + 3.3	0.742	0.460
Tumor CT value (HU)	60.1 + 16.6	62.0 + 17.6	0.603	0.548
LSLN (mm)	20.5 + 9.2	17.8 + 10.0	1.592	0.114
SSLN (mm)	13.9 + 7.5	11.9 + 8.7	1.415	0.159
No. of lymph nodes	6.4 + 3.8	4.8 + 3.0	2.792	0.006
Preoperative CT				
Tumor thickness (mm)	13.2 + 6.5	10.5 + 4.5	2.572	0.012
Tumor length (mm)	5.6 + 2.2	5.0 + 2.6	1.471	0.144
Tumor CT value (HU)	51.7 + 17.0	49.0 + 16.5	0.933	0.353
LSLN (mm)	16.6 + 6.0	13.4 + 5.9	3.03	0.003
SSLN (mm)	11.4 + 5.3	8.0 + 4.4	3.946	<0.001
No. of lymph nodes	7.9 + 4.6	5.5 + 3.6	3.356	0.001
Change after chemotherapy				
Tumor thickness change (mm)	4.4 + 4.6	6.7 + 4.9	2.651	0.009
Tumor length change (mm)	2.0 + 1.7	2.3 + 2.4	0.655	0.513
Tumor CT value (HU)	8.4 + 15.5	13.0 + 14.5	1.738	0.085
LSLN change (mm)	3.9 + 5.7	4.4 + 6.3	0.406	0.686
SSLN change (mm)	2.6 + 4.6	3.8 + 6.1	1.267	0.208
No. of lymph node change	1.5 + 1.9	0.7 + 1.6	2.565	0.012

LSLN indicates long axis size of maximum lymph node; SSLN, short axis size of maximum lymph node.

*The value of the data was means ± standard deviation. The *P* value was from independent-samples T test.

these biological behavior factors should be taken into account in comprehensively predicting LNM.

Other machine-learning methods have been used in medical studies. The mainly used method is artificial neural network (ANN), which is considered an appropriate tool for medical data analysis.[28] Bollschweiler et al applied a single-layer perceptron, an ANN, to predict lymph node metastasis in esophageal cancer, with an accuracy of 79%.[29] However, the ANN has some disadvantages: (1) the model is prone to overfitting, (2) it requires lengthy development and optimization time, and (3) it is more difficult to use in the field because of computational requirements.[30] Considering the above reasons, this study instead selected the SVM model, which could produce lower prediction error compared with classifiers based on other methods like artificial neural networks.[31] Compared with ANN, SVM may have the same or even better predictive ability.[32,33] Few reports are available regarding the application of SVM in esophageal cancer lymph node metastasis. In this preliminary study, the results indicated that the SVM model has better diagnostic capability for LNM than the traditional LN size criteria, with AUC achieving a good diagnostic power. With further improvement, SVM may become an effective tool in predicting lymph node staging in esophageal cancer.

Our study has some limitations. First, although a relatively large sample size was used, this was a single-center retrospective study. Further prospective studies are warranted to confirm the diagnostic power of the SVM model. In addition, the majority of patients were male (77.9%). Gender factors may influence the external validity of these findings. Finally, the AUC obtained for the LS-SVM model in the testing sample was relatively lower

TABLE 3. AUC of CT Indicators

AUC	AUC	SE	95% CI
Thickness on pCT	0.620	0.0505	0.531 to 0.703
LSLN on pCT	0.666	0.0485	0.579 to 0.746
SSLN on pCT	0.705	0.0466	0.619 to 0.782
Number of LN on pCT	0.669	0.0484	0.581 to 0.749
Number of LN on bCT	0.636	0.0505	0.547 to 0.718
Thickness change	0.634	0.0496	0.545 to 0.716

bCT indicates baseline CT; pCT, preoperative CT; LSLN, long axis size of maximum lymph node; SSLN, short axis size of maximum lymph node.

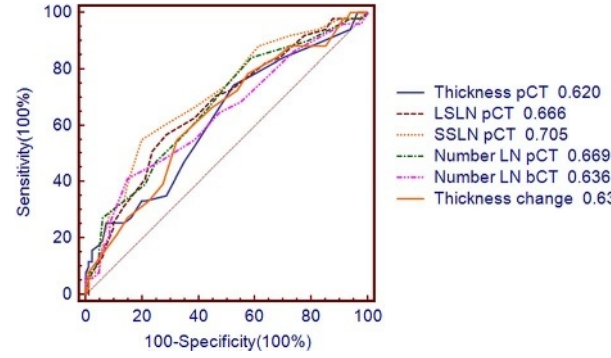

FIGURE 2. Receiver operating characteristic (ROC) curve for lymph node metastasis with six CT indicators. The highest AUC of these six CT indicators was 0.705 which was performed by the short axis size of maximum lymph node (SSLN) of preoperative CT. Figure 2 can be viewed online in color at www.jcat.org.

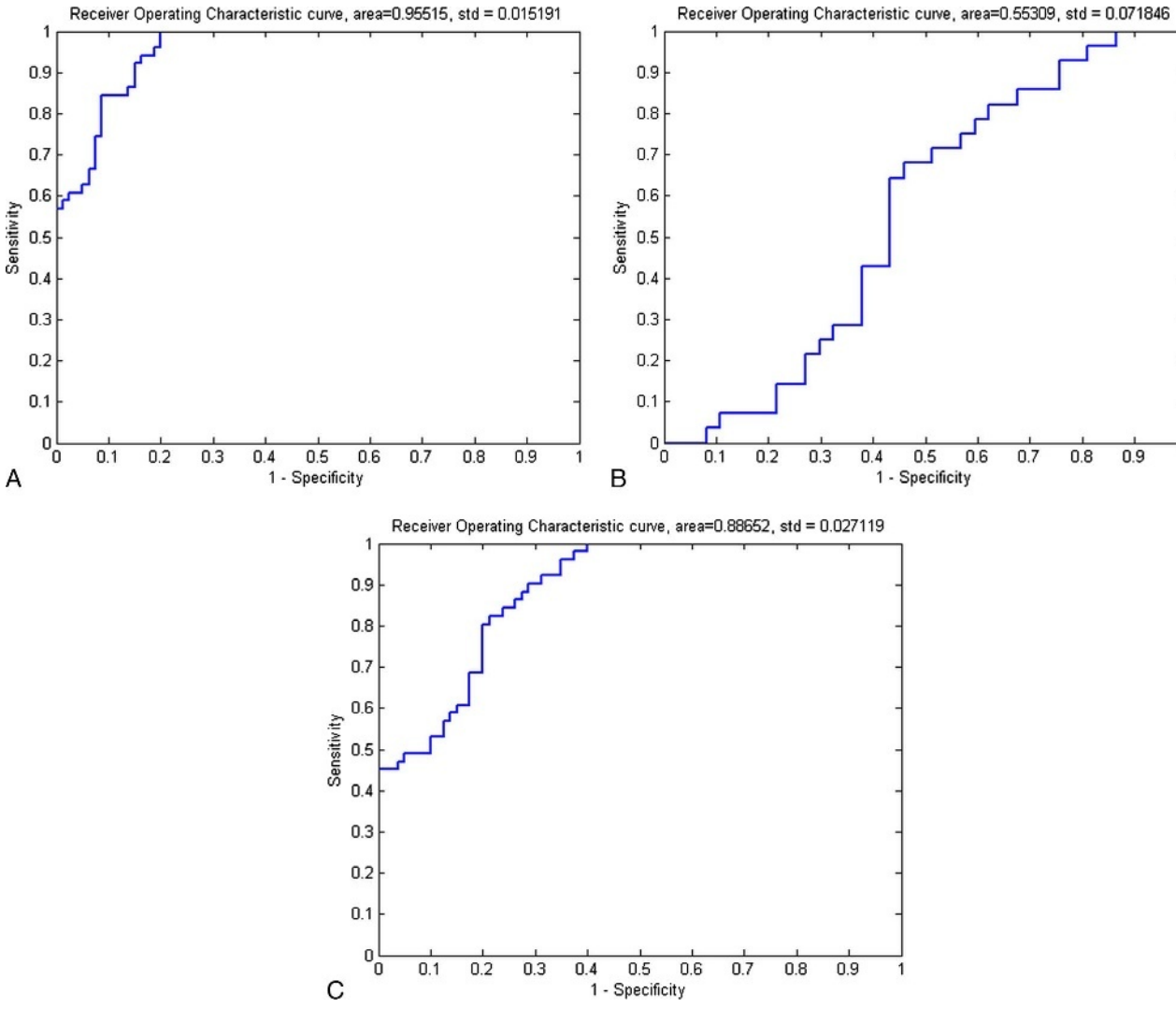

FIGURE 3. (A–C) Receiver operating characteristic (ROC) curve for lymph node metastasis with LS-SVM model. A, The AUC of the model predicting training sample was 0.955. B, The AUC of the model predicting testing sample was 0.553. C, The AUC of the SVM model predicting all samples reached 0.887. Figure 3 can be viewed online in color at www.jcat.org.

compared with the training sample value. This indicates a need for improvement of the model's ability to assess new cases.

CONCLUSIONS

The least squares support vector machine model based on CT images can help diagnose lymph node metastasis in esophageal cancer with preoperative chemotherapy.

ACKNOWLEDGMENTS

We thank Jie Li, Kun Cao, Lei Tang, Yong Cui, Li-Ping Qi, and Shun-Yu Gao for editorial support and Jun Shan, Ning Wang, Ying Li, Xiao-Yan Zhang, and Yan-Ling Li for reviewing the manuscript.

REFERENCES

1. Lerut T, De Leyn P, Coosemans W, et al. Surgical strategies in esophageal carcinoma with emphasis on radical lymphadenectomy. *Ann Surg*. 1992; 216:583–590.
2. Siewert JR, Bartels H, Bollschweiler E, et al. [Squamous cell cancer of the esophagus. Treatment concept at the surgical clinic of the Munich Technical University]. *Chirurg*. 1992;63:693–700.
3. Watanabe H. [Squamous cell cancer of the esophagus. Treatment concept at the National Cancer Center in Tokyo]. *Chirurg*. 1992;63: 689–692.
4. Roth JA, Pass HI, Flanagan MM, et al. Randomized clinical trial of preoperative and postoperative adjuvant chemotherapy with cisplatin, vindesine, and bleomycin for carcinoma of the esophagus. *J Thorac Cardiovasc Surg*. 1988;96:242–248.
5. Swisher SG, Hunt KK, Holmes EC, et al. Changes in the surgical management of esophageal cancer from 1970 to 1993. *Am J Surg*. 1995; 169:609–614.
6. Müller JM, Erasmi H, Stelzner M, et al. Surgical therapy of oesophageal carcinoma. *Br J Surg*. 1990;77:845–857.
7. Hulscher JB, van Sandick JW, de Boer AG, et al. Extended transthoracic resection compared with limited transhiatal resection for adenocarcinoma of the esophagus. *N Engl J Med*. 2002;347: 1662–1669.

8. Hagen JA, DeMeester SR, Peters JH, et al. Curative resection for esophageal adenocarcinoma: analysis of 100 en bloc esophagectomies. *Ann Surg*. 2001;234:520–530.
9. Hofstetter W, Swisher SG, Correa AM, et al. Treatment outcomes of resected esophageal cancer. *Ann Surg*. 2002;236:376–384.
10. van Hagen P, Hulshof MC, van Lanschot JJ, et al. Preoperative chemoradiotherapy for esophageal or junctional cancer. *N Engl J Med*. 2012;366:2074–2084.
11. Ychou M, Boige V, Pignon JP, et al. Perioperative chemotherapy compared with surgery alone for resectable gastroesophageal adenocarcinoma: an FNCLCC and FFCD multicenter phase III trial. *J Clin Oncol*. 2011;29: 1715–1721.
12. Cunningham D, Allum WH, Stenning SP, et al. Perioperative chemotherapy versus surgery alone for resectable gastroesophageal cancer. *N Engl J Med*. 2006;355:11–20.
13. Mariette C, Dahan L, Mornex F, et al. Surgery alone versus chemoradiotherapy followed by surgery for stage I and II esophageal cancer: final analysis of randomized controlled phase III trial FFCD 9901. *J Clin Oncol*. 2014;32:2416–2422.
14. Rice TW, Rusch VW, Apperson-Hansen C, et al. Worldwide esophageal cancer collaboration. *Dis Esophagus*. 2009;22:1–8.
15. Xu Y, Jiang Y, Yu X, et al. Analysis of new N-category on prognosis of oesophageal cancer with positive lymph nodes in a Chinese population. *Radiol Oncol*. 2013;47:63–70.
16. Wakelin SJ, Deans C, Crofts TJ, et al. A comparison of computerised tomography, laparoscopic ultrasound and endoscopic ultrasound in the preoperative staging of oesophago-gastric carcinoma. *Eur J Radiol*. 2002; 41:161–167.
17. Yu W, Liu T, Valdez R, et al. Application of support vector machine modeling for prediction of common diseases: the case of diabetes and pre-diabetes. *BMC Med Inform Decis Mak*. 2010;10:16.
18. Klöppel S, Stonnington CM, Barnes J, et al. Accuracy of dementia diagnosis: a direct comparison between radiologists and a computerized method. *Brain*. 2008;131(pt 11):2969–2974.
19. Das K, Giesbrecht B, Eckstein MP. Predicting variations of perceptual performance across individuals from neural activity using pattern classifiers. *Neuroimage*. 2010;51:1425–1437.
20. Mourão-Miranda J, Bokde AL, Born C, et al. Classifying brain states and determining the discriminating activation patterns: Support Vector Machine on functional MRI data. *Neuroimage*. 2005;28:980–995.
21. Suykens J, Vandewalle J. Least squares support vector machine classifiers. *Neural Process Lett*. 1999;9:293–300.
22. Bishop C. *Pattern recognition and machine learning*. Springer; 2006. http://www.springer.com/cn/book/9780387310732.
23. Yokota T, Igaki H, Kato K, et al. Accuracy of preoperative diagnosis of lymph node metastasis for thoracic esophageal cancer patients from JCOG9907 trial. *Int J Clin Oncol*. 2016;21:283–288.
24. Kim TJ, Kim HY, Lee KW, et al. Multimodality assessment of esophageal cancer: preoperative staging and monitoring of response to therapy. *Radiographics*. 2009;29:403–421.
25. Dorfman RE, Alpern MB, Gross BH, et al. Upper abdominal lymph nodes: criteria for normal size determined with CT. *Radiology*. 1991;180:319–322.
26. Fultz PJ, Feins RH, Strang JG, et al. Detection and diagnosis of nonpalpable supraclavicular lymph nodes in lung cancer at CT and US. *Radiology*. 2002; 222:245–251.
27. Picus D, Balfe DM, Koehler RE, et al. Computed tomography in the staging of esophageal carcinoma. *Radiology*. 1983;146:433–438.
28. Patel JL, Goyal RK. Applications of artificial neural networks in medical science. *Curr Clin Pharmacol*. 2007;2:217–226.
29. Bollschweiler EH, Mönig SP, Hensler K, et al. Artificial neural network for prediction of lymph node metastases in gastric cancer: a phase II diagnostic study. *Ann Surg Oncol*. 2004;11:506–511.
30. Ahmed FE. Artificial neural networks for diagnosis and survival prediction in colon cancer. *Mol Cancer*. 2005;4:29.
31. Byvatov E, Schneider G. Support vector machine applications in bioinformatics. *Appl Bioinformatics*. 2003;2:67–77.
32. McQuisten KA, Peek AS. Comparing artificial neural networks, general linear models and support vector machines in building predictive models for small interfering RNAs. *PLoS One*. 2009;4:e7522.
33. Lee HJ, Hwang SI, Han SM, et al. Image-based clinical decision support for transrectal ultrasound in the diagnosis of prostate cancer: comparison of multiple logistic regression, artificial neural network, and support vector machine. *Eur Radiol*. 2010;20:1476–1484.